Paper

Electrode Shape Design at the Power Cable Joint by Using $(\mu + \lambda)$-ES Multi-Objective Evaluation

Daigo Yonetsu* Student Member
Takehisa Hara* Member
Shigeki Shimada** Non-member
Mikio Kaji** Member

This paper proposes effective and general-purpose insulation design method of the power cable joint. To improve the insulation performance of the cable joint, the electric field strength on the inner electrode surface should be made as low as possible. The evolution strategy (ES) method is employed for obtaining the optimum shape of the electrode. The multi-objective evaluation is performed as well as the single-objective evaluation. The one of the objective functions is the maximum electric field strength on the electrode and the other is the maximum electric field strength along the interface. The electrode shape that shows the smallest maximum electric field is obtained among the shapes that satisfy the constraint condition.

Keywords: power cable joint, optimum design, surface charge method, evolution strategy, multi-objective evaluation

1. Introduction

To improve the insulation performances of the power cable joint, it is necessary to make the electric field strength on the inner electrode surface as low as possible [1] [2]. The constraint condition is that the electric field strength along the interface between insulation rubber and XLPE lies within the range of the permissible value. Experimental design method has been usually employed for designing the power cable joint [3]. In this case, the expected shape can be obtained after a few iterations. However, it is difficult to obtain the exact optimum shape, because the obtained shape depends on the selection of design parameters (for example, the curvature radii and the lengths of the electrode).

The object of our research is to establish a general-purpose and exact insulation design method of the power cable joint. There are two-type methods for performing the electric field optimization: gradient methods [4] [5] and direct search methods [6] [7]. Gradient methods can reduce the objective function effectively because it employs the derivatives of the objective function. However, the obtained shape depends on the initial shape and the search is apt to fall into the local minimum. On the other hand, direct search methods do not depend on the initial shape and can widely search the optimum shape. Moreover, they can insert the constraint condition into the objective function easily.

Then, we examine the electric field optimization by using the evolution strategy method $(\mu + \lambda)$-ES [8] [9] that is one of the direct search method. The symbol μ presents the number of the parent individuals and the symbol λ presents that of the offspring individuals. The μ parents create the λ offspring by cross-over and mutation and $(\mu + \lambda)$-ES individuals compete for survival. Therefore, the $(\mu+\lambda)$-ES can search the optimum shape widely and locally. The surface charge method that provides accurate solutions on the boundaries for the multi-layer substances with relatively small number of elements is employed for the calculation of the electric field distribution. The second order of Riesenfeld spline function [10] is applied for modeling the inner electrode contour. Riesenfeld spline curve is not only smoothly drawn by a few control points, but also can connect the neighboring line smoothly and continuously.

First, we attempt the single-objective evaluation. The maximum electric field strength on the electrode is chosen as the objective function. In the case where the maximum electric field along the interface exceeds the permissible value, the objective function is increased and the shape is made hard to survive as the optimum one.

Next, we attempt the multi-objective evaluation [11]. One of the objective functions is the maximum electric field strength on the electrode, and the other is that along the interface. The multi-objective evaluation is performed in order not to fall into the local minimum. The search results by multi-objective evaluation are compared with those by single-objective evaluation.

2. Electric Field Analysis at the Power Cable Joint

2.1 Structure of the Power Cable Joint

Fig. 1 shows the structure of the power cable joint that is so called SPJ (Self-Pressurized Joint) [1]. The

* Kansai University
3-3-35, Yamate-cho, Suita 564-8680
** Sumitomo Electric Industries
1-7, Hikaridai, Seika-cho, Soraku, Kyoto 619-0237

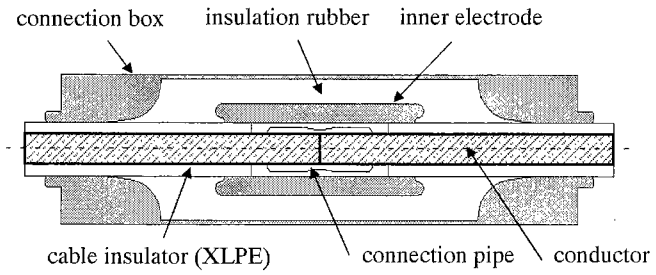

Fig. 1. A structure of power cable joint

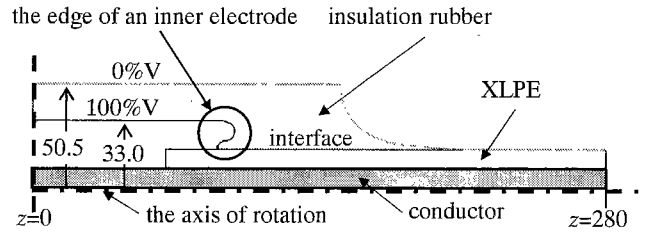

Fig. 2. A cross section of power cable joint used for analysis

end parts of two XLPE cables are connected each other by connection pipe. XLPE cables are fixed by interface pressure that is generated by contraction of insulation rubber. In such a power cable joint, it is necessary to reduce the electric field strength on the inner electrode and that along the interface between insulation rubber and XLPE.

2.2 Analytical Model Fig. 2 shows a cross section of the power cable joint used for analysis. The analytical model considers axial symmetry and symmetry of the joint configuration. The relative permittivities of insulation rubber and XLPE are 2.5 and 2.3, respectively. The radii of conductor and XLPE are 10.5 mm and 19.0 mm, respectively.

The surface charge method is employed for the electric field calculation. The shape for each element is expressed by a line and the surface charge density on each element is defined by the first order expression. All the elements are less than 2.5 mm length and the elements on the inner electrode and those along the interface between insulation rubber and XLPE are chosen more finely. The total number of elements is 687. Natural boundary condition ($E_n = 0$) [12] is employed at $z = 0$ and $z = 280$. Eight-point Gaussian quadrature rule is employed as numerical integration. The complete elliptic integral of the first kind and that of the second kind is calculated by means of Landen transformation [13]. The solution for the simultaneous equation is performed by Bi-CGSTAB method [14].

2.3 Modeling of the Inner Electrode Contour Fig. 3 shows the contour shape of the inner electrode to be optimized. Design parameters are z-coordinates from control points P_3 to P_6 and r-coordinates from control points P_2 to P_5. The coordinates of control points P_1 and P_7 are fixed. The inner electrode contour is expressed by the second order of Riesenfeld spline function that interpolates between the seven control points. The second order of Riesenfeld spline curve

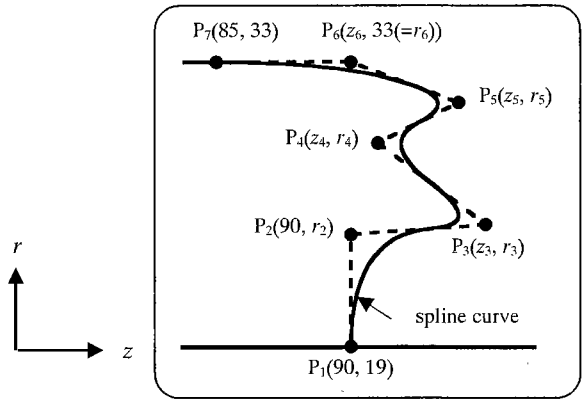

Fig. 3. The inner electrode contour composed of Riesenfeld spline curves

meets tangentially to the line that connects two adjacent control points at the center of the line and is tangent at its end-points to the first and last line segments. Then, the r-coordinate of the control point P_6 is chosen equal to that of the control point P_7 so that the spline curve is smoothly connected at the control point P_7. The z-coordinate of the control point P_2 is chosen equal to that of the control point P_1 so that the inner electrode should be perpendicular to the cable insulator (XLPE). In order to make the inner electrode contour shape always smooth, the range of each the control point is set as the followings.

$$\left.\begin{array}{ll} 90 \le z_i \le 110 & (i = 3 \sim 5) \\ 85 < z_6 \le 110 & \\ 19 < r_i \le r_{i+1} \le 33 & (i = 2 \sim 5) \end{array}\right\} \cdots\cdots\cdots (1)$$

As another method of expressing the electrode shape smoothly, modeling by arcs is considered. In this case, though the insulation design is performed efficiently [15][16], the optimization needs the experiential knowledge to decide the direction of the arcs. The constraint condition to connect continuously the electrode contour becomes complicated. In the case of the method described in this paper, it is not necessary to consider the above mentioned considerations. Furthermore, the spline method can express more various shapes than the arc method.

3. Optimization Method

3.1 Setting of Single-objective Function The electrode shape optimization is performed by $(\mu + \lambda)$-ES. The optimization procedure is shown in chapter 3.3. The optimum condition is to reduce the maximum electric field strength on the inner electrode. The constraint condition is to keep the maximum electric field strength along the interface between insulation rubber and XLPE below a permissible value. Then, the objective function for each individual (shape) is given as a following equation in the case of single-objective evaluation.

$$f = \begin{cases} E_{c\_\max} & (E_{i\_\max} \le E_{i\_\mathrm{per}}) \\ E_{c\_\max} + 100(E_{i\_\max} - E_{i\_\mathrm{per}}) & \\ & (E_{i\_\max} > E_{i\_\mathrm{per}}) \end{cases} \cdots\cdots\cdots\cdots (2)$$

where $E_{c\_\max}$ is the maximum electric field strength obtained in the optimization process on the inner electrode, $E_{i\_\max}$ is that along the interface between insulation rubber and XLPE and E_{i_per} is a permissible value for $E_{i\_\max}$. By means of Eq. (2), the individual on which the maximum electric field strength along the interface exceeds a permissible value is made hard to survive as the optimum shape though the maximum electric field strength on the inner electrode is small.

3.2 Setting of Multi-objective Functions On the case of multi-objective evaluation, the two objective functions for each individual (shape) are given as a following equation.

$$\left.\begin{aligned} f_1 &= E_{c\_\max} \\ f_2 &= E_{i\_\max} \end{aligned}\right\} \quad \cdots\cdots\cdots\cdots\cdots\cdots\cdots\cdots\cdots\cdots \quad (3)$$

Fonseca's ranking method [11] is employed for evaluating the two objective functions. The rank of each individual, $rank(x_j)$ is given as,

$$rank(x_j) = 1 + n_j \quad (j = 1 \sim \mu + \lambda) \cdots\cdots\cdots (4)$$

where j is the iteration number for parent individuals and offspring individuals, n_j presents the number of individuals of which the two objective functions are smaller than those of individual j. The number of parent individuals (μ) is set as 30 and that of offspring individuals (λ) is set as 100. Eq.(4) indicates that the smaller rank is, the more individual is preserved to the next generation. As the optimization progresses, the individuals whose two objective functions are smaller together are apt to be obtained.

However, there is a possibility that the individuals are distributed too widely or too locally. Then, the evaluation is improved as shown in Fig. 4. The permissible zone which the individuals exist is limited so that the individuals do not distribute too widely. The range of the permissible zone is between 90% and 110% of the permissible value for the second objective function f_2. The individual which exceeds the permissible zone is never preserved to the next generation. Next, the permissible zone is divided into thirty zones and the only one individual exists in each zone so that the individuals are distributed homogeneously. In each zone, the individual whose rank is smallest is preserved to the next generation. If there are many individuals whose rank is equal to each other, the individual whose first objective function f_1 is smallest is preserved. For example, the symbol "•" presents the individual which is preserved to the next generation, the symbol "✕" presents the individual which is dumped into the dustbin in Fig. 4.

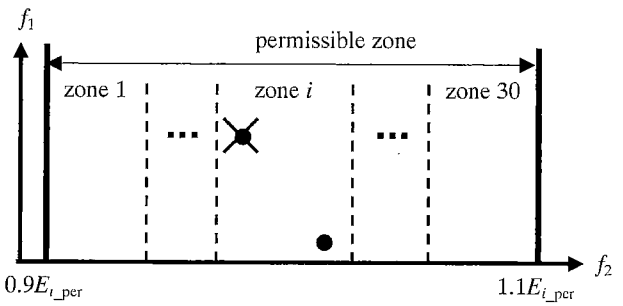

Fig. 4. Preservation of individuals

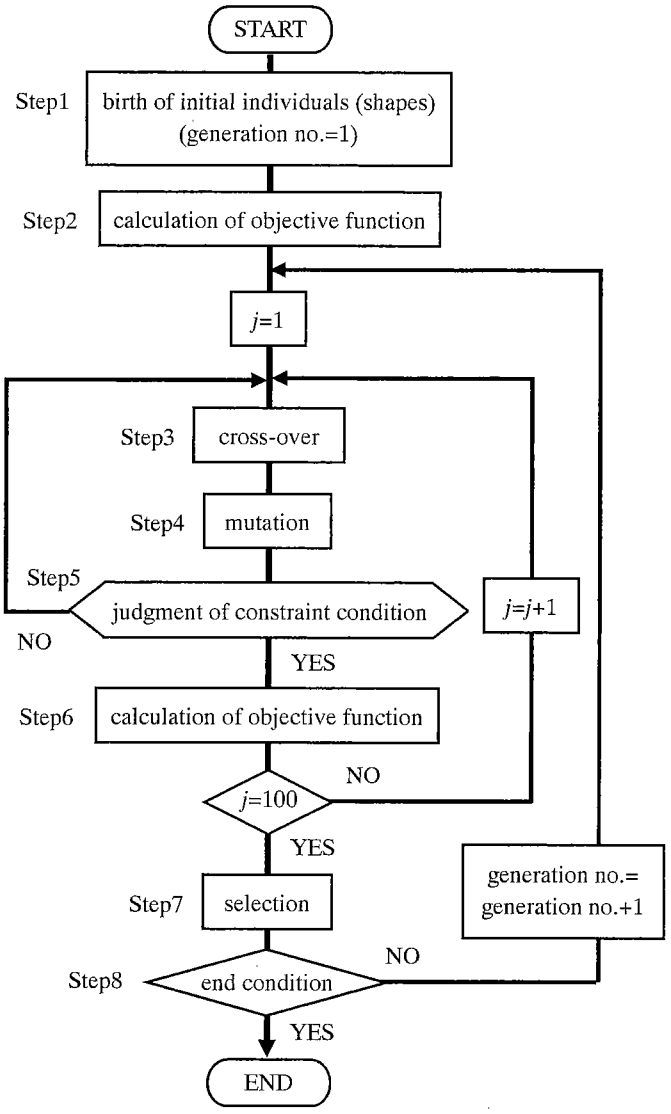

Fig. 5. Optimization procedure by $(\mu+\lambda)$-ES

3.3 Optimization Procedure by $(\mu + \lambda)$-ES

Flow diagram of the electrode shape optimization procedure by $(\mu+\lambda)$-ES is shown in Fig. 5. The optimization procedure of every step is shown as follows.

[Step 1] birth of initial individuals (shapes): The thirty individuals are generated randomly as the initial generation. However, all the initial individuals satisfy Eq. (1).

[Step 2] calculation of objective function: After the electric field calculation by using the surface charge method, the objective functions for each individual are calculated by Eq. (2) in the case of single-objective evaluation and by Eq. (3) in the case of multi-objective evaluation.

[Step 3] cross-over: The two individuals are arbitrary selected from the thirty parent individuals. Taking $\boldsymbol{x}_{p1}$ and $\boldsymbol{x}_{p2}$ for the two parameter vectors which are arbitrary selected, the component of parameter vector for offspring individual, $\boldsymbol{x}_{c,i}$ is set as,

$$x_{c,i} = x_{p1,i} + rnd \times (x_{p2,i} - x_{p1,i}) \quad (i = 1 \sim 8) \quad \cdots\cdots\cdots\cdots\cdots\cdots (5)$$

where i is the repeat number for design parameters and rnd is uniform random number from 0 to 1. Eq. (5) presents that the dividing point between $\boldsymbol{x}_{p1}$ and $\boldsymbol{x}_{p2}$ is selected as the parameter vector for offspring individual. Here, design parameters are truncated a number to two decimal places.

[Step 4] mutation: After operating Step 3, The mutation is performed by the following equation.

$$x_{c,i} = x_{c,i} + N_i(0, \sigma) \quad \cdots\cdots\cdots\cdots\cdots\cdots\cdots\cdots (6)$$

where $N_i(0, \sigma)$ is normalized random number for each design parameter whose average is 0 and the standard deviation is σ. The setting of the standard deviation for each design parameter is the same in magnitude so as to adjust easily.

[Step 5] judgment of constraint condition: The offspring is judged whether Eq. (1) is satisfied or not. If the offspring individual vector obtained by operating Step 3 and Step 4 does not satisfy the Eq. (1), the operation returns to Step 3.

[Step 7] selection: The thirty individuals are preserved among parent individuals and offspring individuals by the evaluation method mentioned in chapter 3.1 and chapter 3.2 and they become the next parent individuals.

[Step 8] end condition: If the standard deviation becomes less than 5.0×10^{-3}, the optimization is terminated. The initial value of standard deviation is taken 5.0 and the value is multiplied by 0.93 as the generation number increases. The standard deviation is adjusted automatically under ordinary $(\mu+\lambda)$-ES [8] [9]. However, the $(\mu + \lambda)$-ES used in this paper does not consider the auto-adjustment of the standard deviation in order to perform the optimization in the constant iteration number (9930 times).

4. Optimization Results

4.1 Result of Single-objective Evaluation

First, the single-objective optimization by using $(\mu + \lambda)$-ES is attempted. For comparison, the oblong electrode contour is set as the standard shape. Fig. 6 shows the search process for the best case and the worst case among ten trials. Here, the maximum electric field strength on the inner electrode is normalized by that of the standard shape(E_{c0_max}) and that along the interface between insulation rubber and XLPE is normalized by the permissible value(E_{i_per}). As a result, the maximum electric field strength on the inner electrode is reduced as the iteration number increases. The maximum electric field strength along the interface converges to the permissible value (1.0). The obtained electric field distributions on the inner electrode and those along the interface are shown in Fig. 7 and Fig. 8, respectively. The maximum electric field values in the best case and worst case are 59.1% and 61.5% of the standard case, respectively. It is seen from Fig. 8 that the maximum electric field strength for both cases are almost equal to the

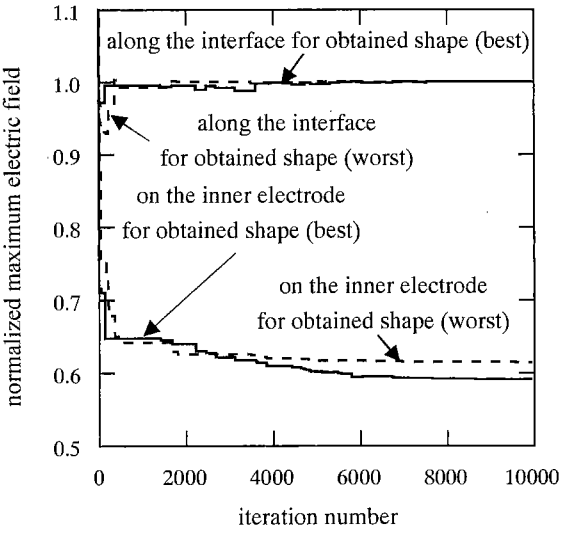

Fig. 6. Maximum electric field variation versus iteration number (single-objective case)

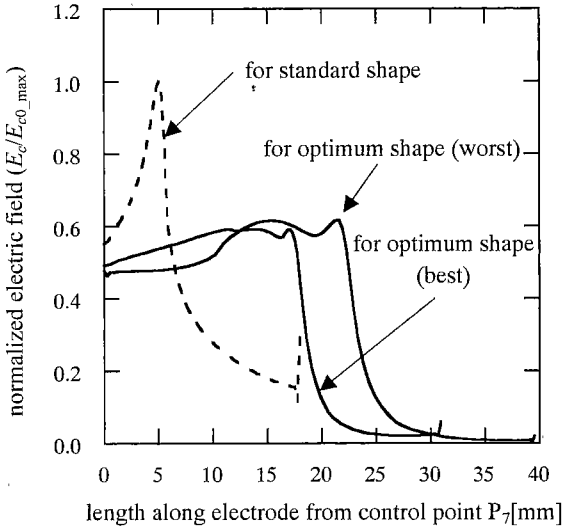

Fig. 7. Electric field distribution on the inner electrode (single-objective case)

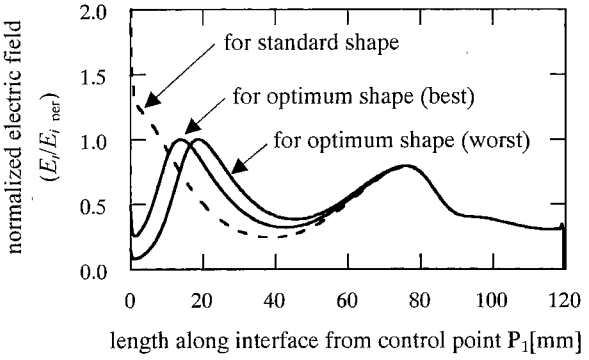

Fig. 8. Electric field distribution along the interface between insulation rubber and XLPE (single-objective case)

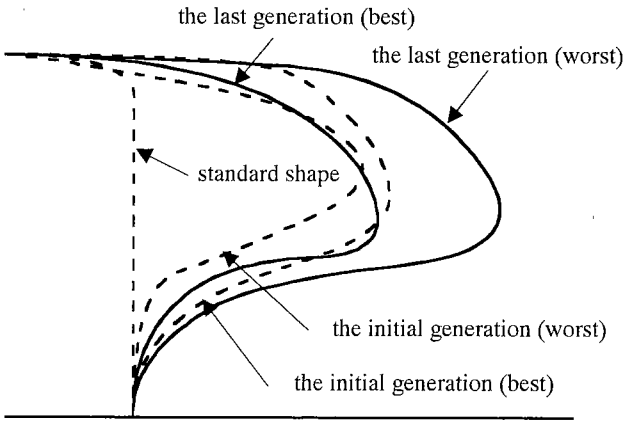

Fig. 9. The optimum electrode shape compared with the standard shape (single-objective case)

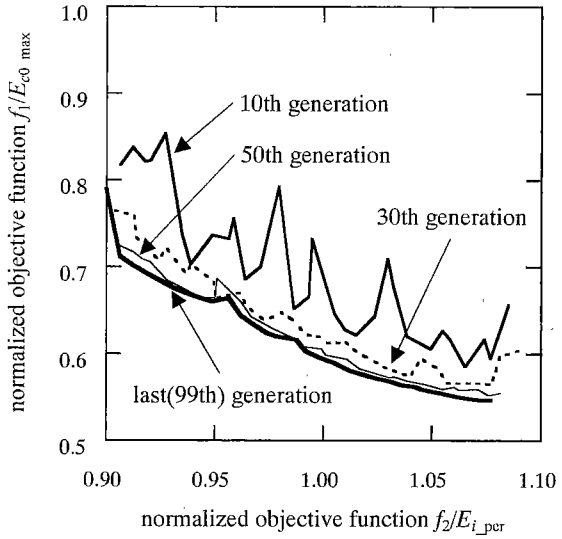

Fig. 10. Objective functions variation for several generation number

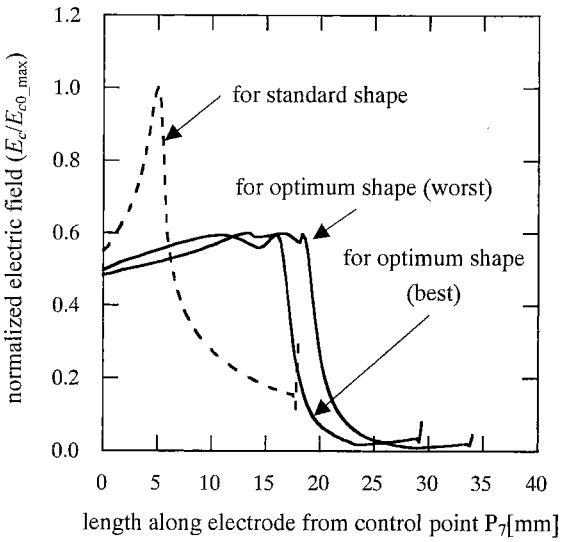

Fig. 11. Electric field distribution on the inner electrode (multi-objective case)

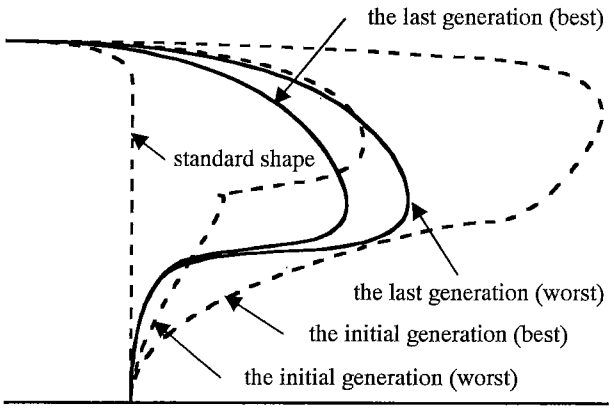

Fig. 12. The optimum electrode shape compared with the standard shape (multi-objective case)

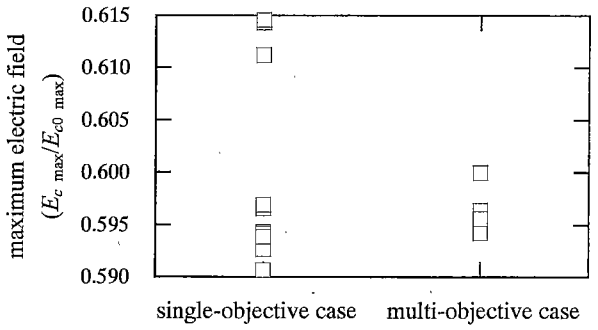

Fig. 13. Distributions of the maximum electric field for ten trials

permissible value. Fig. 9 shows the obtained optimum electrode contours at the initial generation and those at the last generation. The obtained electrode contours at the last generation are different from those at the initial generation. It is thought that the obtained contour at the last generation does not depend on that at the initial generation.

4.2 Results of Multi-objective Evaluation

Next, multi-objective optimization is attempted as well as the single-objective optimization. The search process in the case of multi-objective optimization is same as the case of single-objective optimization that is shown in Fig. 6. The objective functions variation for several generation numbers is shown in Fig. 10. It is seen from Fig.10 that the two objective functions of parent individuals surely decrease as the generation number increases. The individual of which the maximum electric field strength on the inner electrode is the smallest among the individuals that satisfy the constraint condition, is selected as the optimum shape. The calculated electric field distributions on the inner electrode and the electrode shapes are shown in Fig. 11 and Fig. 12, respectively. Both Fig. 11 and Fig. 12 are the same results as the case of single-objective optimization. However, the difference between the best and the worst case is smaller than that in the case of single-objective optimization. The maximum electric field for the best case is 59.4% and for the worst case 60.0% of the standard shape, respectively. The maximum electric field strengths along the interface are less than the permissible value in both cases.

4.3 Comparison of Results by Two Methods

The search results for the case of single-objective

optimization and those for the case of multi-objective optimization are compared. Fig. 13 shows distributions of the maximum electric field strength on the inner electrode for ten trials. It is seen from Fig. 13 that the difference among ten trials for the case of multi-objective optimization is smaller than that for the case of single-objective optimization. Furthermore, all of the results of multi-objective optimization show small maximum electric field, though the best result is obtained in the case of single-objective optimization. It is thought that the searches sometimes fall into the local minimums in the case of the single-objective optimization. Meanwhile, searching shapes in the case of the multi-objective optimization are distributed widely and it is possible that the searching shapes escape the local minimum. It takes about 11.4 hours to perform the optimization for each trial. The personal computer with 1.0 gigabytes of memory and Intel Pentium III 800 MHz of CPU is used.

5. Conclusions

In this paper, the electrode shape optimization at the power cable joint is attempted by using the surface charge method and the $(\mu + \lambda)$-ES. The results are the following:

(i) By using the second order of Riesenfeld spline function for expressing the inner electrode contour, the optimum shape design can be performed easily and the obtained inner electrode contour has smooth shape.

(ii) Both single-objective and multi-objective evaluations can achieve the desirable insulation design; the maximum electric field strength on the inner electrode takes almost lowest value and that along the interface between insulation rubber and XLPE is within the permissible value.

(iii) The search results of the multi-objective evaluation are far better than those of single-objective evaluation. The difference between the best case and the worst case of the multi-objective evaluation is smaller than that of single-objective evaluation and the search is stable.

As mentioned above, the $(\mu + \lambda)$-ES employing multi-objective evaluation is proved to be effective and general-purpose method for insulation design at the joint of power cable. This optimization method is thought to be applicable to insulation design for other high-voltage power apparatuses. We should like to thank Dr. Y. Yasuda, a Lecturer of the Department of Electrical Engineering, Kansai University for his helpful comments and encouragement. This work is partially supported by Kansai University HRC project of "Development and Characterization of Sensor and Actuator for Micro Robot".

(Manuscript received March 3, 2003,
revised July 28, 2003)

References

(1) K. Fudamoto, S. Yamada, S. Narisada, H. Satoh, and K. Mizunami: "Development of Compact type Straight Through Joint for High Voltage XLPE Cable", The Papers of Technical Meeting on Electric Cable and Wire, IEE Japan, EC-99-5, pp.25–29 (1999)

(2) T. Ito, S. Nakagawa, A. Kuwaki, T. Hashio, and T. Shiono: "Interfacial Phenomena in Composite Electrical Insulation—Evaluation of Directed Electrical Field Strength at Interfaces of the Prefabricated Joint Model—", The Papers of Technical Meeting on Electric Cable and Wire, IEE Japan, EC-99-2, pp.7–12 (1999)

(3) A. Kuwaki, K. Ito, and A. Arai: "Study on interface insulation design of a prefab junction for CV cables", The Papers of Technical Meeting on Dielectrics and Electrical Insulation, IEE Japan, DEI-94-36, pp.51–59 (1994)

(4) H. Tsuboi and T. Misaki: "Optimization of Electrode and Insulator Contours by Using Newton Method", *T. IEE Japan*, Vol.106-A, No.7, pp.307–314 (1986)

(5) H. Tsuboi and T. Misaki: "The Optimum Design of Electrode and Insulator Contours by Nonlinear Programming Using the Surface Charge Simulation Method", *IEEE Trans. Magnetics*, Vol.24, No.1, pp.35–38 (1988)

(6) Y. Hosokawa, S. Noguchi, and H. Yamashita: "Optimal Design for Permanent Magnet Motor", The Papers of Technical Meeting on Static Apparatus and Rotating Machinery, IEE Japan, SA-99-19, RM-99-73, pp.33–38 (1999)

(7) T. Ohnishi and N. Takahashi: "Investigation of Optimal Design of IPM Motor using Finite Elements and Optimization Technique", *T. IEE Japan*, Vol.121-D, No.3, pp.397–402 (2001)

(8) K. Preis, C. Magele, and O. Biro: "FEM AND EVOLUTION STRATEGIES IN THE OPTIMAL DESIGN OF ELECTROMAGNETIC DEVICES", *IEEE Trans. Magnetics*, Vol.26, No.5, pp.2181–2183 (1990)

(9) T. Nagao: Optimization Algorithms, Chapter 10, pp.136–150, Shokodo, Japan (2000)

(10) R.H. Bartels, J.C. Beatty, and B.A. Barsky: An Introduction to Splines for use in Computer Graphics and Geometric Modeling, Chapter 12, pp.261–291, Morgan Kaufmann Publishers, America (1987)

(11) C.M. Fonseca and P.J. Fleming: "Genetic Algorithms for Multiobjective Optimization: Formulation, Discussion and Generalization", Proc. of 1st International Conference on Genetic Algorithms and Their Applications, pp.93–100 (1985)

(12) S. Sato, W.S. Zaengl, and A. Knecht: "A NUMERICAL ANALYSIS OF ACCUMULATED SURFACE CHARGE ON DC EPOXY RESIN SPACER", *IEEE Trans. Electrical Insulation*, Vol.EI-22, No.3, pp.333–340 (1987)

(13) S. Sato: "Effective Calculation Technique for the Complete Elliptic Integrals", *T. IEE Japan*, Vol.116-A, No.10, pp.897–898 (1996)

(14) R. Barrett, M. Berry, T.F. Chan, J. Demmel, J. Donato, J. Dongarra, V. Eijkhout, R. Pozo, C. Romine, and H. van der Vorst: "Templates for the Solution of Linear Systems: Building Blocks for Iterative Methods", Chapter 2, pp.6–48, Asakura Shoten, Japan (1996)

(15) D. Yonetsu, T. Hara, S. Shimada, and M. Kaji: "OPTIMUM ELECTRODE CONTOUR DESIGN AT THE JOINT OF POWER CABLES", Proc. of The JSST 2000 International Conference on Modeling, Control and Computation in Simulation, pp.342–345 (2000)

(16) D. Yonetsu, T. Hara, S. Shimada, and M. Kaji: "Examination of Electric Field Optimization at the Joint of Power Cables", *Simulation*, Vol.21, No.1, pp.51–56 (2002)

Daigo Yonetsu (Student Member) was born on June 28, 1975. He received the B.S. and the M.S. degrees in electrical engineering from Kansai University in 1998 and 2000, respectively. He is presently a doctoral student at graduate school of Kansai University. His current subject of research is electric field optimization of power apparatus.

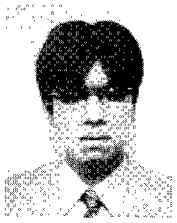

Takehisa Hara (Member) was born on February 18, 1943. He received the Ph.D. degree from Kyoto University in 1970. He joined as a research associate and an associate professor at the department of electrical engineering, Kyoto University in 1970 and 1975, respectively. Since 1997, he has been with the department of electrical engineering, Kansai University as a professor. His current subject of research is optimization simulation for electric apparatus design, electromagnetic analysis in apparatuses and plasma, surge overvoltage analysis and insulation design in electric power system and so on. He was awarded excellent paper awards from IEEJ in 1974 and from Japan Society for Simulation Technology in 1993, respectively. He is a member of Japan Society for Simulation Technology, the Institute of Electrical Installation Engineers of Japan, Institution of Energy and Resource.

Shigeki Shimada (Non-member) received the B.S. and the M.S. degrees in electronic engineering from Kyoto University in 1995 and 1997, respectively. He entranced Sumitomo Electric Industries, Ltd in 1997. He is presently a research worker at CAE Research Center. His current subject of research and development is simulation in electric power field, simulation for cutting process and so on. He is a member of Japan Society for Simulation Technology.

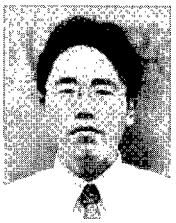

Mikio Kaji (Member) graduated from the department of mathematics, Kyoto University in 1971. He entranced Sumitomo Electric Industries, Ltd. in 1971. He is presently a center chief at CAE Research Center. He is a Doctor of Engineering. His current subject of research and development is FEM in electrical and electronics field, simulation of development process for electronic industry material, simulation for element design, computer graphics, basis network system for research and development. He is a member of Institute of Electrical and Electronics Engineers, The Japan Society of Applied Physics, The Physical Society of Japan, Japan Society for Simulation Technology and The Japan Society for Industrial and Applied Mathematics.